Research Article / Review Article FUPRE JOURNAL 8(2): 106-112 (2024)

FUPRE Journal

of

Scientific and Industrial Research

ISSN: 2579-1184(Print) ISSN: 2578-1129 (Online)

http://fupre.edu.ng/journal

Determination of Subsurface Sewage Contamination of Rocks and Water using 2-D Resistivity Imaging: A Niger delta University Teaching Hospital Case Study, Bayelsa state Southern Nigeria.

ALILE, M. O.[1,*], *OGINI, A. A.* [1]

[1]*Department of Physics University of Benin, Benin City Edo State Nigeria*

ARTICLE INFO

Received: 09/10/2023
Accepted: 21/12/2023

Keywords

Contaminant Migration, Resistivity imaging, Sewage Contamination

ABSTRACT

Septic tanks as used in the management of sewage systems may result to both surface and/or subsurface (groundwater) pollution. While remediation and repairs of surface sewage spillage in septic tanks is feasible, the reverse is the case with subsurface pollution of porous media through sewage seepages. 2-D Electrical Resistivity Imaging (ERT) was used to determine the nature of sewage contamination of subsurface rocks in the premises of the Niger Delta University Teaching Hospital (NDUTH) Okolobiri in Bayelsa State, Southern Nigeria. It was observed that in the presence of contaminant fluids, geoelectrical resistivity signatures behave anomalously in most cases being more conductive than the clean rock/fluid system. Also, that contaminant fluid, in the course of time, finds its way into groundwater to alter the electrical and chemical properties of pristine rock/fluid as seen in this investigation. The observed subsurface contaminant (leachate) migrate in the direction of groundwater flow and decreases in concentration away from the source (septic tank) which in the current study is in the North – South direction as represented in the 2-D resistivity contouring of the three (3) geoelectrical profiles in this report.

1. INTRODUCTION

When incorporated in near surface rocks, biodegradable organic matter of plant and animal origin has been known to be electrically conductive in comparison with pristine adjacent rocks (Reynolds, 2011; Revil and Glover, 1998). A comparative analysis of the resistivity image of the subsurface has potential of yielding useful information on the extent and direction of migration of contaminant plumes (Dey & Morrison, 1979; Al Temamy et al., 2008). In the case of septic tanks for collection of sewage which in practice are located within the limits of the earth's protective layers, the intention is to prevent them from contaminating groundwater on the one hand and also to prevent superficial spillage on the other hand all of which have environmental and health implications. While it is easy to monitor surface leakages in septic tanks, the reverse is the case when underground seepage and/or migration of sewage fluid is involved especially in the midst of saturated porous rocks (aquifers). Though initially slow depending on the fineness and thickness of the protective layer as defined by the Dar Zarouk's parameters, a

*Corresponding author, e-mail: *oginiataman@gmail.com*
DIO

whole body of groundwater can be contaminated within a short period one's sewage leachates find their way into porous water bearing rocks (Nwankwo and Ngah 2014; Okiongbo and Akpofure 2012; Adagunodo and Sumoni, 2012). In consideration of two major facts: (1) that time-bound remediation of in-situ groundwater is yet to be domesticated within the limits of available technologies in sub Sahara Africa, and (2) owing to the fact that water table in the transition and lower Niger delta is expected to exhibit high periodic amplitudes due to increasing rates and frequencies of seasonal floods occasioned by climate change; preventing our aquifers from man induced contaminations such as sewage, landfill and oil spills cannot be over emphasized. Electrical resistivity tomography provides a useful means of viewing or monitoring sewage seepage and migration of similar electrically detectable underground contaminant fluids (Bayowa et al., 2012; Olawuyi, 2012). A similar scheme has been used to map the extent of underground oil spill pollution in parts of the coastal plain of Lagos Nigeria (*Wasiu et al., 2018). The intention in this study is to run and analyze resistivity profiles along or close to preexisting septic tanks with a view to distilling useful information on the patterns of subsurface contaminant fluid migration.

1.1 Location of Study

The study area is located on Latitude 5^0 1' 50" N and 5^0 2' 5"N and Longitude 6^0 18' 55"E and 6^0 19' 10" E within the premises of the Niger Delta University Teaching Hospital Okolobiri-Bayelsa State in Niger Delta Southern Nigeria.

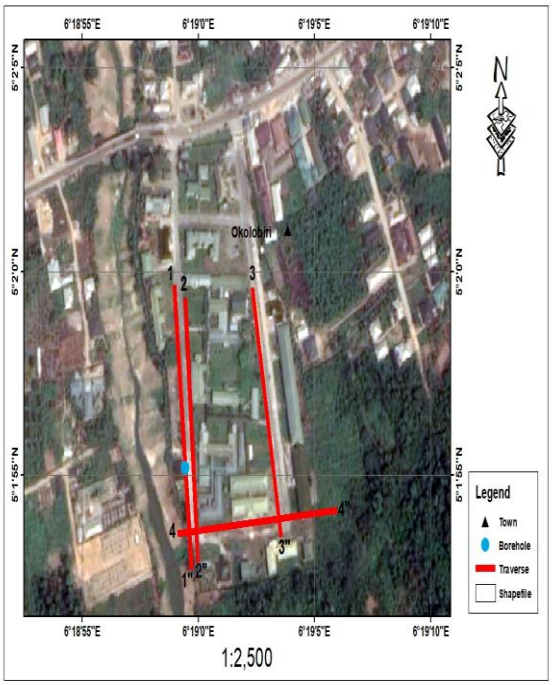

Figure 1: Google Earth Satellite Imagery showing 2D survey profiles at the Niger Delta University Teaching Hospital (NDUTH) Okolobiri.

1.2. Theoretical Foundation of Method

Resistivity is often first encountered in physics when discussing the resistance of an ideal cylinder of length 'L' and cross-sectional area 'A' of uniform composition. The resistivity appears as the material's specific constant of proportionality in the expression for the total resistance of the cylinder (Herman et al., 2001). Figure 2 is a simplified cylindrical conductor of length 'L' and cross sectional area 'A', the direction of current flow is as indicated by the arrow.

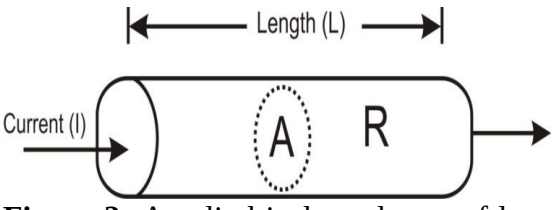

Figure 2: A cylindrical conductor of length L and cross sectional area A.

Thus;

$$R = \frac{\rho L}{A} \quad (1)$$

Eqn. (1) relates the electrical resistance of the cylindrical conductor to its physical dimension without considering the potential difference causing the flow of electric current. The constant of proportionality (ρ) is intrinsic to the nature of the material and represents it's reluctance to the passage of electric current. But taking the potential difference causing current flow into account, then resistance 'R' is expressed from Ohm's law.

$$R = \frac{V}{I} \quad (2)$$

Comparing (1) and (2)

$$\frac{\rho L}{A} = \frac{V}{I} \quad (3)$$

$$\therefore \rho = \left(\frac{V}{I}\right)\left(\frac{A}{L}\right) \quad (4)$$

'V' is expressed in volts while 'ρ' is in (Ωm)

V/I measures the apparent resistance of the cylinder $\mathbf{R}_{app}$; and A/L referred to as the geometric factor **K** carries information about the geometry of the cylinder.

Our simplified expression for resistivity on the basis of the forgoing becomes;

$$\rho = \boldsymbol{R}app * \boldsymbol{K}(\Omega\text{m}) \quad (5)$$

The model of equation (5) is true in simple terms, yet it falls short of requisite mathematics to establish the physical link between resistivity and electrical potential as a function of distance from a point source in an earth material when the earth's dimension is not in practice restricted to regular shapes (cylinder). To resolve this, we recall the vector form of Ohm's law from electromagnetic theory (Herman et al., 2001; Flathe and Leibold, 1976).

$$J = \frac{1}{\rho} * E = -\frac{1}{\rho} * \nabla V \quad (6)$$

'J' is the current density vector (ampere/m^2), 'E' the electric field intensity (volts/m^1), V is electric potential (volts) and ∇ the del operator.

Next, we consider a point current source on a homogenous half space of earth material with uniform resistivity. This constitute a better approximation since the air- surface boundary is assumed to have an infinite resistivity and current spreads downward into the earth along a semi sphere defined by equipotential surfaces with radius 'r' from the point source (figure 3).

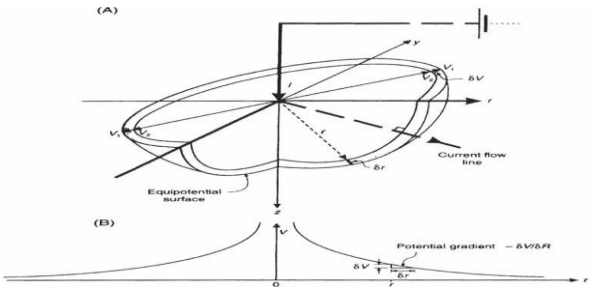

Figure 3: (A) point current source on a homogeneous hemispherical half space of uniform resistivity. (B) Graph of potential gradient with increasing 'r' (adapted from Reynold 2011)

∇V In equation 6 expresses the potential gradient which according to figure 2B decreases away from the point source along equitotential surfaces of expanding radius as the negative sign implies.

With the parameters of figure 3, we rewrite (6) thus:

$$\frac{I}{2\pi r^2} = -1/\rho\left(\frac{\partial V}{\partial r}\right)$$

Where $\frac{I}{2\pi r^2}$ is the current density and $\frac{\partial V}{\partial r}$, the potential gradient

So that;

$$-\frac{I\rho}{2\pi r^2}\partial r = \partial V$$
$$V = -I\rho/2\pi \int \frac{1}{r^2}\,\partial r$$
$$V = \frac{I\rho}{2\pi r} + C \quad (7)$$

Where C represents the arbitrary constant of integration

The partial derivative is used to replace the increment $\frac{\delta V}{\delta r}$ where r can be evaluated along any preferred coordinate axis. Equation 7 gives the potential at any point of our homogenous half space earth material with respect to a single point source.

For a source and sink i.e. a two electrode system where current goes into the ground through one electrode and returns to the surface at the second electrode, the difference in potential can be evaluated by integrating within the limits r_1 and r_2 (figure 4).

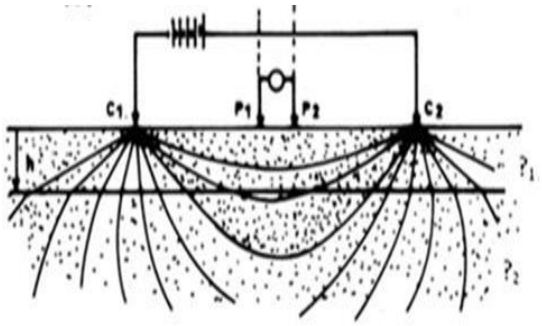

Figure 4: A bipolar arrangement with source and sink at C_1 and C_2 respectively (after Flathe et and Leibold, 1976)

With reference to figure 4, we determine the difference in potentials (ΔV) due to C_1 and C_2 respectively along any point of the equipotential current flow lines;

Thus;

$$\Delta V = \frac{I\rho}{2\pi}\,[1/r_1 - 1/r_2] \quad (8)$$

$$\rho_a = 2\pi\left[\frac{1}{r_1} - \frac{1}{r_2}\right]^{-1} \times \frac{\Delta V}{I} \quad (9)$$

Again observe that $2\pi\left[\frac{1}{r_1} - \frac{1}{r_2}\right]^{-1}$ contains information about the geometry of our homogenous half space earth material as well as the spatial arrangement of the bipolar electrode system, hence constitutes another way of expressing the geometric factor of equations (4) and (5). While $(\frac{\Delta V}{I})$ defines the earth's resistance

$$\rho_a = \mathbf{K.R}\ (\Omega\text{m}) \quad (10)$$

It is interesting to note that we have arrived back at equation (5) and the resistivity is assumed apparent because in practice, the earth is not homogeneous which calls for some level of filtering/inversion to arrive at what can be accepted as a representation of the earth's true resistivity.

2. MATERIAL AND METHOD

Pasi earth resistivity meter model 16GL-N was used, a modern optimal instrument with technical specifications that enhanced the reliability of field results as evident in the following technical details: 16 bit floating point with signal sensitivity of 600 nV and 126 nA; capable of averaging signals 3 times before final output in each cycle of measurement, and suppresses noise up to 96 dB at 50-60 Hz with instrument-range automatic adaptation to observable field signals using automatic filtering all managed by a multiprocessor.

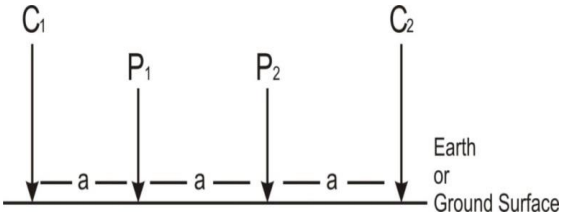

(a)

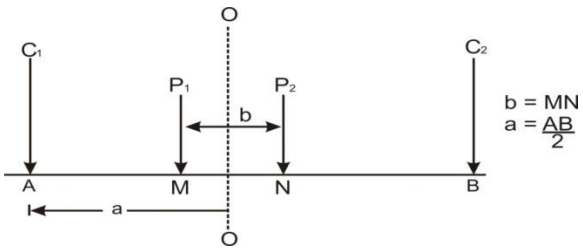

(b)

Figure 5: (a) Wener array; (b) Schlumberger array.

Combined Wener-Schlumberger survey geometry was employed using a 21 electrode system with dipole spacing of 10m (figure 5). Four (4) reels of wire were used; two potential and two current electrode wires each provided with crocodile clips at the ends. 2D field geoelectric resistivity survey procedures as prescribed by Loke (2004) was used wherein the instrument recorded voltage and currents as input signals and outputs resistance (R) measurable in ohms. It took about 5 - 90 seconds for the instrument to complete 3 cycles of a single reading, and exactly 90 individual instrument readings to generate data that completely covers a single 2D profile.

Data processing

From equation (10), the data processing task was basically the multiplication of instrument field resistance '**R**' recordings with a geometric factor '**k**' representing the influence of the earth's geometry with respect to the acquisition array on the observed field recordings (Kearey & Brooks, 1991; Dobrin, 1976; Al Tamamy, et al., 2008). The multiplication of instrument reading '**R**' and the geometric factor '**k**' for each field observation produced an apparent resistivity value of the subsurface layer under investigation.

$$\rho_a = KR$$

Where ρ_a is apparent resistivity (Ωm)

R is the resistance (Ω) of the subsurface obtained from surface readings and

K, the geometric factor which according to (Loke, 2004) is given by the formula;

$$K = \pi n(n+1)a\,. \qquad (11)$$

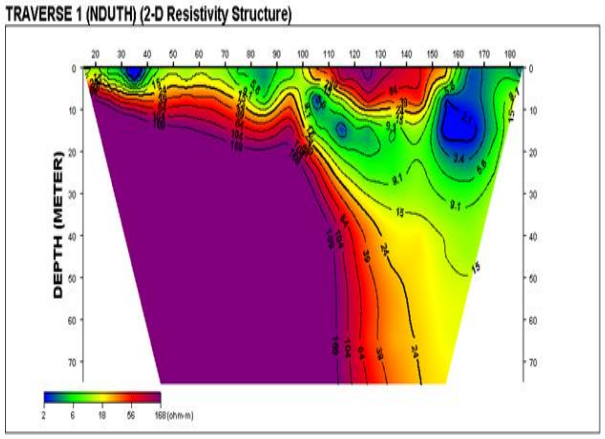

Figure 6: 2-D Resistivity Structure of Traverse 1 (NDUTH)

3. RESULTS AND DISCUSSION

3.1. Results Presentation

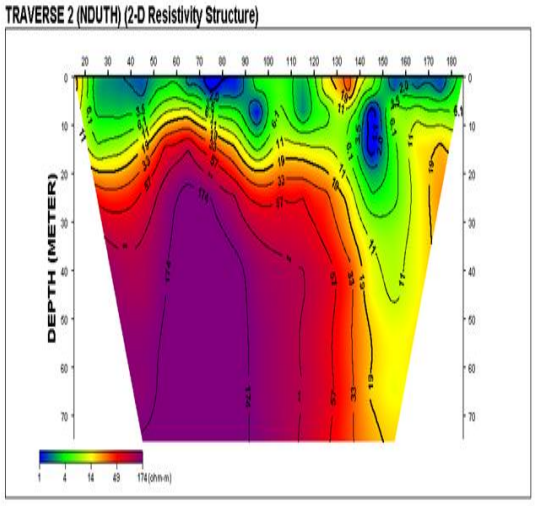

Figure 7: 2-D Resistivity Structure of Traverse 2 (NDUTH)

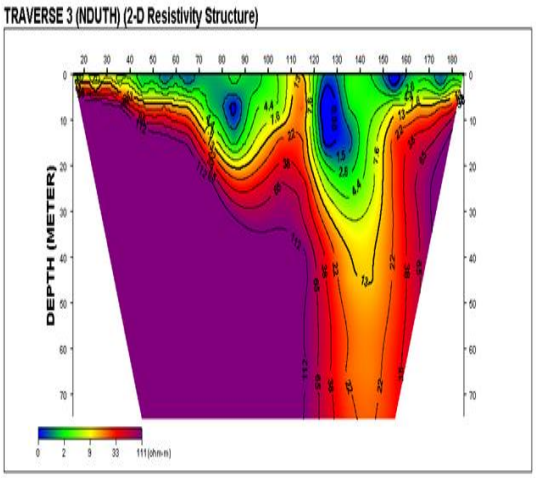

Figure 8: 2-D Resistivity Structure of Traverse 3 (NDUTH)

3.2. Discussion

From the resistivity profile of Traverse-3 (figure 8), it could be seen that what would have appeared as a uniform resistivity structural contour with maximum resistivity value of about 112 Ωm running horizontally at about 10 m of depth is obscured and pushed down beyond the limits of the survey resolution at the right side of the profile accounting for a prolonged and deep contaminant fluid migration at this point. Also, the purple colour of the 112 Ωm contour appears to continue away from the right margin of the profile indicating that northward migration is restricted. The low resistivity material corresponded to the positions of the septic tanks located between the 140 m and 150 m electrode positions. In figure 7, the migration of leachate is shown by the anomalous resistivity contour behavior with increasing resistivity values away from the source. The above observed pattern aided the delineation of two (2) near surface low resistivity closures which corresponded to the two (2) septic tanks located close to the profile of traverse-2 between the 80^{th} and 90^{th} electrode positions, and between the 160^{th} and 170^{th} electrode positions (figure 7). On the other hand, traverse-1 has only one (1) septic tank where the migrating leachate manifested as a low resistivity material ranging between 1.0 Ωm to about 15 Ωm (figure 6). Again, the North – South fading out of low resistivity contours depictive of the direction of contaminant fluid migration was observed.

4. CONCLUSION

In conclusion, it was observed that while leachate from septic tanks gradually permeate the groundwater, it also migrate in sympathy to the direction of groundwater flow. Again, that sewage contamination manifests as anomalous resistivity low in comparison to the surrounding rocks and decrease in concentration away from source (septic tanks) by an observed fading out of low resistivity contour into the more stable or uniform structures of the clean formation. The uncontaminated subsurface rocks and fluids tend to exhibit uniform electrical characteristics along any subsurface horizon as evident in the three (3) reported geoelectrical profiles. This approach of electrical resistivity application has proved useful in groundwater development plans

References

Adagunodo, T. A. and Sunmonu, L. A., (2012). Geoelectrical assessment of groundwater prospect and vulnerability of overburden aquifers at Adumasun Area,Oniye, Southwestern Nigeria. Archives of Applied Science Research, 4(5), 2077-2093

Al Temamy, A. M. M., Mohamed, A. K. and Mostafa, S. M. B. (2008). Use of geo-electrical techniques to determine the impact of facies changes on groundwater potential and water logging in the area south of Lake Manzala, Nile delta, Egypt. Egyptian Journ of Desert Research (58) 2, 1 – 18.

Bayowa, O. G., Dele, E. F., Martin, O. O. and Adekule, A. A., (2012). Groundwater Contamination Prediction Using Finite Element Derived Geoelectric Parameters Constrained by Chemical Analysis around a Sewage site, South-western Nigeria. International Journal of Geosciences, 3, 404-409.

Dey, A. and Morrison, H. F., (1979). Resistivity modelling for arbitrary shaped 2-dimensional structures. Geophysical Prospecting, 27, 1020 – 1036.

Dobrin, M.B., (1976). Introduction to geophysical prospecting, 3rd ed., McGrawHill, New York.

Flathe, H. and Leibold, W., (1976). The Smooth Sounding Graph: a manual for field work in direct current resistivity sounding. Federal Institute for Geosciences and Natural Resources, Hannover/Germany.

Herman, J.R., Celarier, E., and Larko, D., (2001). UV 380 reflectivity of the earth's surface, clouds and aerosol journal of geophysical research, vol 106.

Kearey P., and Brooks, M., (1991). An Introduction to Geophysical Exploration, Blackwell science limited, London. Pg 281

Loke, M. H., (2004). Tutorial: 2-D and 3-D electrical Imaging surveys.

Nwankwoala, H.O and Ngah, S.A., (2014). Groundwater resource of the Niger Delta: Quality implication and management consideration. Internal journal of water resource and environmental engineering, 6(5), 155-165.

Okiongbo, K. S., and Akpofure, E., (2012). Determination of Aquifer Properties and Groundwater Vulnerability Mapping using Geoelectric Method in Yenagoa city and its Environs in Bayelsa state, south-South Nigeria. Journal of Water Resource and Protection, (4), pp. 354-362.

Olawuyi, A. K., (2012). Geo-electrical Exploration of Groundwater within the Premises of University of Illorine Teaching Hospital, Kwara State, Nigeria. NJTD, 9(2): 120 – 127.

Reynolds, J. M., (2011). An Introduction to Applied and Environmental Geophysics 2nd ed. Wiley BlackWell Publication, UK.

Revil, A. and Glover, P.J.W., (1998). Nature of Surface Electrical Conductivity in Natural Sands, Sandstones and Clays. Geophysical Research letters, 25(5), 691-694.